Comparison of Heat and Mass Transport at the Micro-Scale

E. Holzbecher, S. Oehlmann

Georg-August Univ. Göttingen

*Goldschmidtstr. 3, 37077 Göttingen, GERMANY, eholzbe@gwdg.de

Abstract: Phenomena of heat and mass transfer are often compared, in various porous media applications. Questions of practical interest are, for example, if tracers can be used for the prediction of heat flow, or vice versa if heat can be utilized as, possibly retarded, tracer for predicting the migration of contaminants, nutrients or other substances. Using numerical modelling in artificial porous media we compute heat and mass transport for pore length scales in the range of micrometers. The simulations show different behaviour for heat and for mass, which is due to the different values of the relevant parameters (high Lewis number) and the different physics of transport in the solid phase.

Keywords: Heat and mass transport, thermal conductivity, molecular diffusion, micro-scale modeling, Navier-Stokes equations

1. Introduction

The analogy of heat and mass transfer in porous media is often utilized for the examination of artificial or natural porous systems. It is proposed to use tracer tests for the characterization of geothermal reservoirs [1, 2]. In fact, in a continuum approach for porous media the differential equations describing heat transport on one side or mass transport on the other side are identical in their mathematical appearance. Comparison of the parameters that determine the coefficients of the differential equations, show that heat transfer can be conceived as transport of a retarded substance. The 'heat retardation factor' R can be calculated using the formula

$$R = (\rho C)_b / \theta (\rho C)_f \qquad (1)$$

where $(\rho C)_b$ and $(\rho C)_f$ denote the heat capacities of the bulk material and the fluid, and θ denotes the porosity [3,4].

Vice versa the same approach can be utilized in order to characterize mass transport, when observations concerning heat transport, i.e. temperature measurements, are available [5].

The described convenient analogy between heat and mass transport can only be exploited in continuous systems, that means in particular when the scale of the pore size is much smaller than the scale of interest. In this paper we are concerned with systems in the mm to dm scale with pores in the micro-scale. Under these conditions the validity of the continuity approach is questionable.

In the mentioned range of length scales heat and mass transfer differ in two major respects. First, the parameters for heat and for mass diffusion differ by a factor of 10^3 (= Lewis number := thermal diffusivity / molecular diffusivity). Second, heat transfer occurs in fluid and solid phase, while mass transfer processes are relevant in the pore space only. Using pore scale modeling we take both these differences into account, in order to examine if the analogy holds still.
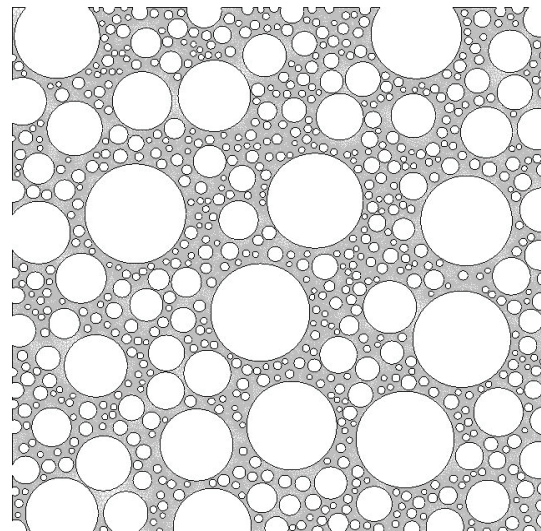

Figure 1. Example of an artificial porous medium, consisting of spheres of different size, as used in the numerical experiments; finite element mesh of the pore space for flow and mass transport modeling

2. Numerical experiments

Numerical experiments are performed in 2D artificial porous media. Using MATLAB® we construct a porous medium consisting of non-

intersecting spheres of different size, using a random number generator for positions and diameters of the spheres.

The user of the code specifies a minimum and a maximum radius, as well as a minimum distance between spheres. The area is filled until a specified porosity is reached. One example geometry is depicted in Figure 1.

The produced geometry is used for varying length scales L for the entire domain. For this study we took a minimum length of 1 mm and a maximum length of 100 mm. It turns out that this is an interesting scale range for the aim of this study. Corresponding pore spaces are in the range of μm. This is indeed a typical scale for pore spaces in many natural or artificial porous media. We chose a minimum of $L = 1$ mm, because with pores at the nano-scale other effects may have to be considered, and our approach would not be valid any more. We chose a maximum of $L = 100$ mm, because at the larger scale, i.e. for larger pore spaces turbulence may come into play, which also is outside the scope of our modelling approach. In fact some test runs with $L = 1$ m led to convergence problems, which are due to the fact that the Navier-Stokes approach is not appropriate anymore, when turbulence comes into play [6].

The parameters for flow as well as for heat and mass transport are chosen in a typical range for a typical porous medium and water at 20°C (see for example: [7]). The values are gathered in Table 1 in the appendix. For porosity only a relatively high value was selected. That is due to the fact that the filling of the porous medium with relatively small solid spheres, as described above, led to problems with execution time, in the MATLAB® program as well as in the COMSOL simulation.

The heat retardation factor according to formula (1) is typically in the range of 2.7.

3. Use of COMSOL Multiphysics

Our model approach is built as follows:

- Solution of Navier-Stokes equations in pore space (stationary)
  - No slip boundary condition at pore surfaces
  - Pressure difference applied by boundary conditions

- Solution of advection-diffusion equation for mass transport in pore space (transient)
  - Using molecular diffusivity as diffusion parameter
  - Concentration specified at inflow; no diffusive flux at outflow
- Solution of convection-conduction equation for heat transport in pore space and in porous medium (two subdomains) (transient)
  - Temperature specified at inflow; no diffusive flux at outflow

Note that we use molecular diffusion as diffusivity parameter in the mass transport model. The more general dispersion approach does not have to be considered here, as that becomes necessary only as a result of the heterogeneous processes in the pore space. Here the pore space is explicitly considered and in pure fluid molecular diffusion is relevant only. Note also that the molecular diffusivity in most systems is three orders of magnitude lower than the mean thermal diffusivity. Using the values from Table 1 the Lewis number amounts to Le= 368, only, which is due to the high porosity.
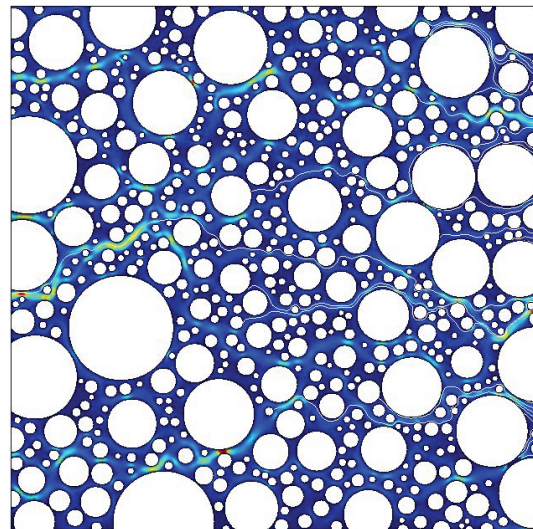

Figure 2. Typical flow field in an artificial porous medium; in color see velocity magnitude (red=high, blue=low), calculated solving Navier-Stokes equations in pore space

Material properties were selected as constant, as we do not intend to restrict this study to a particular temperature or concentration range. Thus the coupling between flow and transport is

not considered (see [8]). Additional effects according to this coupling could emerge due to

- viscosity changes, mostly induced by temperature gradients
- fluid density changes, induced by temperature or salinity gradients

Density changes are usually much smaller in their relative size than viscosity changes. However, in the vertical direction they effect the buoyancy, for which even small-size changes can have a significant impact [8].

Concerning the flow we apply a pressure gradient from one side of the model domain to the other. The pressure difference thus scales linearly with L. On the two remaining boundaries we require a no flow condition. For transport we specify a Dirichlet condition at the inflow boundary, the typical 'no diffusive flux' condition at the outflow boundary, and no-flow transport conditions at the two no-flow boundaries. For transport the initial condition is a constant value in the entire domain that is different from the value specified in the Dirichlet boundary condition.

The finite element mesh for the flow and mass transport calculations is shown in Figure 1: only the pore space is meshed. For heat transfer also the solid spheres are meshed.

4. Results

For each artificial porous medium in a first step the flow field in the pore space is computed as solution of the Navier-Stokes equations. A characteristic output is shown in Figure 2. The pressure drop was applied from the right to the left side. Some preferential flow paths can clearly be observed, as they are characteristic for porous media flow. Aside from the main flow paths the velocity drops to zero rapidly.

Figures 3 and 4 show snapshots of the concentration distribution at selected times, as obtained by the simulations. Snapshot times were selected to ensure that the center of mass is located somewhere the middle of the system. The system represented in Figure 3 has an extension of 1 mm, while the one of Figure 4 has 100 mm. There are already significant differences in both outputs. For the smaller geometry the front is relative homogeneous, while for the larger geometry no single front

position can be recognized. In the former case advection obviously is of minor relevance, while in the latter case advective transport is clearly dominating. This phenomenon is due to the fact that the length scale typical for pore-space in our simulations is also increased. For pipes and channels it is well known that the velocity scales with the second power of the pipe diameter [9]. This also explains that the travel time for the mean mass is shorter in the larger system than in the smaller system.
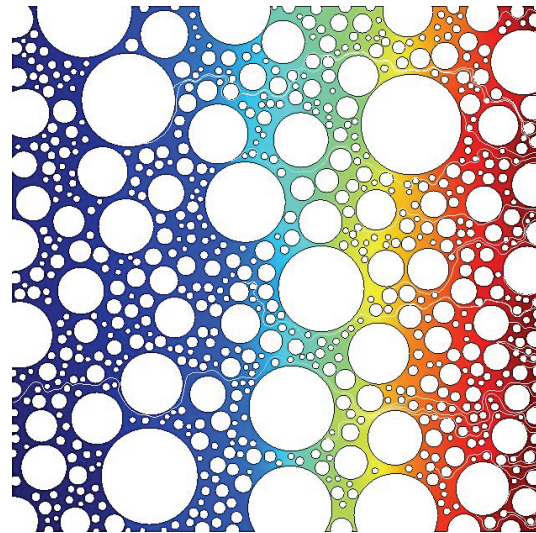

Figure 3. Concentration distribution for mass transport at length L=0.001 m; snapshot at t=800 s
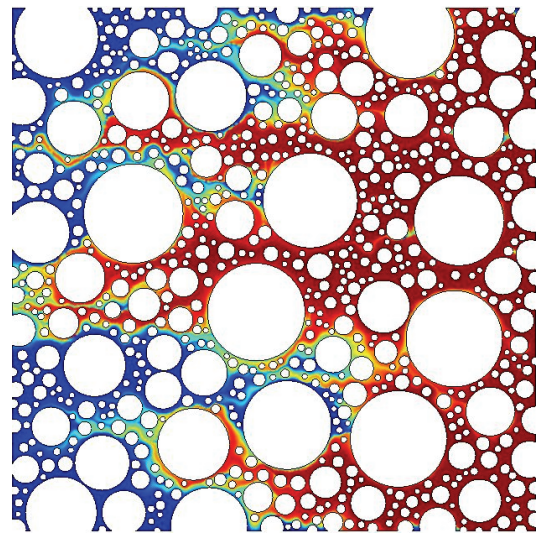

Figure 4. Concentration distribution for mass transport at length L=0.1 m; snapshot at t=230 s
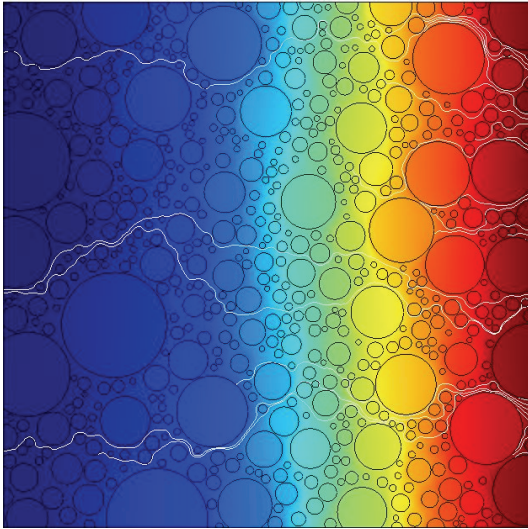
Figure 5. Temperature distribution for heat transport at length L=0.001 m; snapshot at t=1 s
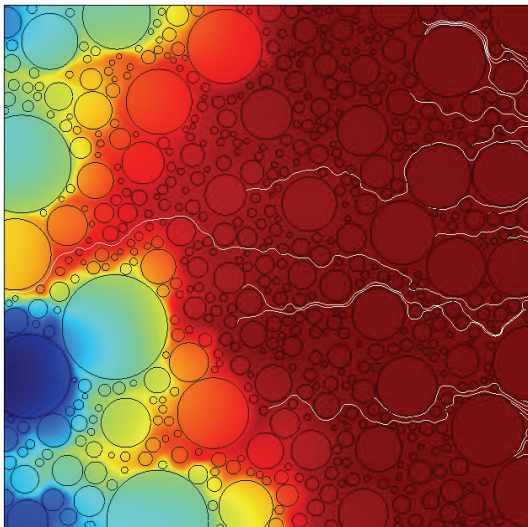

Figure 6. Concentration distribution for mass transport at length L=0.1 m; snapshot at t=500 s

Figures 5 and 6 show snapshots of the temperature distribution at selected times, according to our simulations. Figure 5 is for length extension of 1 mm and Figure 6 for L=100 mm. In the small system one can observe a thermal front, moving with the same velocity independent of the location in transverse direction. However, the travel time is significantly smaller than for mass transport in the corresponding system. The ratio of traveltimes is almost three orders of magnitude, which corresponds with the ratio of diffusivities,

measured by the dimensionless Lewis number. At the small scale either mass or heat transport are diffusion dominated and thus the significant difference in diffusivities becomes crucial.

At the larger length scale heat transport also becomes advection dominated, as it was already observed for mass transport. Figure 6 visualizes that there is no clear front in the system any more, and that the preferential flow paths dominate the transport process. In contrast to mass transport the traveltime t correlates with system length L: traveltime is longer in the larger system.

5. Discussion

Comparison of traveltimes of mass and heat transport shows that a relation:

(1) at the smaller scale mass transport is much slower than heat transport; here the system is diffusion dominated and the ratio of three orders of magnitude in diffusivities becomes crucial.

(2) at the larger scale heat transfer is indeed retarded compared to mass transfer

From the solution for the migration of a front due to pure diffusion (for unknown function c)

$$c(x,t) = c_0 erfc\left(\frac{4Dt}{x^2}\right) \quad (2)$$

follows for the arrival time T of the front at distance L from the source:

$$T = \frac{L^2}{4D\left(erfc^{-1}\left(c/c_0\right)\right)^2} \quad (3)$$

i.e. that the time scales with the square of the length [10]. In contrast the arrival time due to pure advection

$$T = \frac{L}{v} \quad (4)$$

is proportional with L. In advection dominated systems the travel time is nearly proportional to the distance, while in diffusion dominated systems the travel time is proportional to L^2. It is well known that Péclet number 1 characterizes equal arrival times for diffusive and advective transport, which results here for c/c_0=0.5 (approximately).

Which of the arrival times is bigger depends also on the parameters, here the velocity and the

diffusivity. For typical values of groundwater velocity and concerning heat transport the two arrival times are compared in Figure 7.

In the figure one can compare arrival times due to pure diffusion for mass and for heat transport: the two lines ('thermal' and 'solute') increase with a distance representing three orders of magnitude.
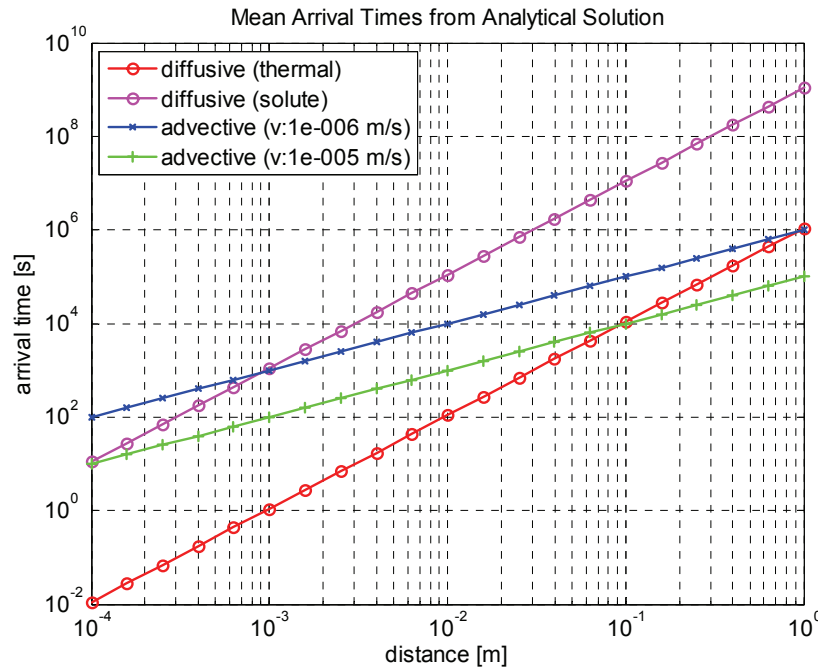

Figure 7. Concentration distribution for mass transport at length L=0.1 m; snapshot at t=500 s

In addition, for two velocities of typical range we show the arrival time according to advection; low velocity in blue and higher velocity in green.

At the microscale at the left side of the graph, thermal diffusion is the fastest process, with arrival time of t=0.01 s for a distance of 0.1 mm. The corresponding arrival time due to molecular diffusion is 10 s (for the calculations here we used a Lewis number Le=1000). If a velocity of 10^{-5}m/s is prescribed, the traveltime due to advection is also 10 s at that scale. Thus for this velocity and length scale diffusion and advection are of equal relevance. For a smaller velocity the system is diffusion dominated as the diffusion arrival time is shorter.

The relations between the different processes change with the distance, as the arrival time curves for diffusion and advection increase with different slope. Thermal diffusion and advection with the higher velocity become equally relevant at 1 dm. For the lower velocity the equality of advection and solute diffusion is reached for 1 mm and of advection and thermal diffusion for 1 m.

These results can not be transferred to the microscale simulations, as parameters are not exactly the same in the analytical derivations and in the numerical simulations. One difference is that in the latter two different thermal diffusivities have to be considered. However the graphs in Figure 7 give some clues for the understanding of the simulations.

The simulations also depend on the type of upscaling of geometry, which is inherently introduced by the procedure of changing scales. Simply changing the length scale by a factor concerns not only the system length scale but also the scale of the pore space. By using this type of up-scaling it is not the same system that is represented at different scales: the larger the system, the larger the pores.

For the general situation other types of upscaling should be considered.

6. Conclusions

If both heat and mass are dominated by diffusion, the relation between heat and mass transport is simple: the significant difference in diffusion parameters makes heat transport much faster than mass transport. This situation can be expected for systems with a length scale lower than 1 mm.

If advection dominates, heat transport in the system can be described as retardation. In the usual velocity range this can be expected for systems larger than 1 m.

In the intermediate range, between 1mm and 1 m system length, there is no simple relation between heat and mass transfer. Due to the differences in diffusivities the transition between a diffusion dominated and an advection dominated regime occurs at different values of L for heat and for mass transport. For a typical velocity range the transition between the regimes may occur at a length scale below 1 mm for heat transport, compared to lengths above 1 dm for mass transport.

In the system length range between few mm and few dm heat and mass transport are hardly to compare, as mass transport is mainly advection dominated, while heat transport is diffusion dominated.

The result is relevant for technical facilities and laboratory experiments, which are typically in the mentioned range. Systems with micro-scale extensions are not concerned, as long as both processes are diffusion dominated. Systems at the (geological) field scale are also not concerned. In particular concerning tracer experiments for the characterization of geothermal energy production, the result is that typical distances should be larger than 1 m. These results are valid for typical low velocities and have to be adjusted if velocity is higher.

7. References

1. Pruess K., van Heel T., Shan C., Tracer testing for estimating heat transfer area in fractured reservoirs, *World Geothermal Congress*, Antalya, Turkey, Proceedings, 8p (2005)
2. Shook G.M., A simple fast method of estimating fractured reservoir geometry from tracer tests, *Trans. Geothermal Resources Council*, **27** (2003)
3. Shook G.M., Predicting thermal breakthrough in heterogeneous media from tracer tests, *Geothermics*, **30**, 573-589 (2001)
4. Ferguson G., Potential use of particle tracking in the analysis of low-temperature geothermal developments, *Geothermics*, **35**, 44-58 (2006)
5. Vogt T., Schirmer M., Cirpka O. A., Investigating riparian groundwater flow close to a losing river using diurnal temperature oscillations at high vertical resolution, *Hydrol. Earth Syst. Sci.*, **16**, 473–487 (2012)
6. Wilcox D.C., *Turbulence Modeling for CFD*, DCW Industries (2006)
7. Häfner F., Sames D., Voigt H.-D., *Wärme- und Stofftransport*, Springer Publ. (1992)
8. Holzbecher E., *Modelling Density-Driven Flow in Porous Media*, Springer Publ. (1998)
9. Guyon E., Hulin J-P., Petit L., *Hydrodynamique Physique*, Ed. du CNRS (1991)
10. Holzbecher E., *Environmental Modeling using MATLAB*, Springer Publ. (2012)

8. Acknowledgements

9. Appendix

Table 1: Parameter values used in model runs

Parameter	Value	Unit
Molecular diffusivity	10^{-9}	m^2/s
Solid thermal diffusivity	$1.29 \cdot 10^{-6}$	m^2/s
Fluid thermal diffusivity	$0.138 \cdot 10^{-6}$	m^2/s
Mean velocity	$0.3 \cdot 10^{-6}$	m/s
Porosity	0.8	1
Fluid density	1000	kg/m^3
Fluid viscosity	0.001	$kg/m/s$